Supporting Information

Akutsu et al. 10.1073/pnas.1015287108

SI Materials and Methods

Cloning and Mutagenesis. A segment of Crimean Congo hemorrhagic fever virus (CCHFV) L-protein comprising the first 217 residues was synthesized by gene synthesis by Mr. Gene Ltd. The original sequence was optimized for codon usage in *Escherichia coli*. From this cDNA, fragments were amplified by PCR and subcloned into the pOPIN-K vector (1) that places a PreScission protease-cleavable glutathione S-transferase (GST) tag at the N-terminus of viral ovarian tumor (OTU) domain of CCHFV (vOTU). Mutagenesis was performed using the QuikChange protocol and primers (Stratagene), but using KOD polymerase (Merck Chemicals) in PCR reactions. The DNA template vector was digested with 1 μL of *Dpn*I for 1 h at 37 °C followed by transformation into Mach-1 (Invitrogen) as per manufacturer manual. Expression constructs for Ub- and ISG15-thioester in the pTYB2 vector were kindly provided by Keith D. Wilkinson (Emory University) and subcloned into pTXB1 vector for higher expression levels. These constructs contain the stabilizing C78S mutation in ISG15. ISG15-C corresponds to residues 79–156.

Protein Expression and Purification. Viral OTU domain construct 1–217 was expressed in *E. coli* B834 strain. For incorporation of seleno-methionine (SeMet), this strain was grown in SelenoMet Medium Base (AthenaES) supplemented with SelenoMet Nutrient Mix and seleno-L-methionine (AthenaES) at 37 °C to an OD_{600} of 0.6, followed by induction with 0.5 mM IPTG and further incubation at 25 °C for 16 h before harvesting. Cells were resuspended and lysed by sonication in Lysis buffer (25 mM Tris, 200 mM NaCl, 5 mM DTT, pH 8.0). After centrifugation (30 min, 40000 × *g*, 4 °C), the cleared supernatant was incubated with Glutathione-S-Sepharose 4B (GE Life Sciences) for 1 h with agitation at 4 °C. The resin was washed with high salt buffer (25 mM Tris, 500 mM NaCl, 5 mM DTT, pH 8.5) and low salt buffer (20 mM Tris, 50 mM NaCl, 5 mM DTT, pH 8.5). The GST-tag was cleaved on the resin with GST-tagged PreScission protease overnight. The cleaved vOTU domain was subjected to anion-exchange chromatography (RESOURCE Q, GE Life Sciences), and further purified by gel filtration (HiLoad 16/60 Superdex 75 column, GE Life Sciences) chromatography in buffer A (20 mM Tris, 200 mM NaCl, 5 mM DTT, pH 8.0). The protein was concentrated to 10 mg/mL. The purity of the protein was >98% judged by SDS-PAGE gel.

Suicide Probe Expression and Purification. pTYB2 and pTXB1 vectors expressing Ub- or ISG15-intein fusion constructs were transformed into Rosetta2 pLacI cells (Novagen), and cells were grown to O.D. 1.0, followed by induction with 0.5 mM IPTG and protein expression at 20 °C overnight. Lysis buffer B (50 mM Hepes, 100 mM NaCl, 100 mM sodium acetate, pH 6.5) was used to resuspend cell pellet and cell lysates were prepared and cleared as described above. Cleared lysate was filtered and incubated with chitin beads at room temperature for 3 h. The beads were washed with 0.5× Lysis buffer B and 0.5× Lysis buffer B containing 550 mM NaCl. Intein cleavage was performed overnight at 4 °C with 200 mM sodium 2-sulfanylethanesulfonate (Mesna). The eluted fractions of free Ub/Ubl thioester were concentrated to 2 mg/mL, buffer exchanged into lysis buffer B, and frozen at −80 °C.

Analytical Ub and ISG15 Suicide Probe Assay. Generation of suicide inhibitors was performed according to published protocols (2). The Ub or ISG15 thioester probes were diluted with lysis buffer B to a final concentration of 1.5 mg/mL. 500 μL of each probe solution was used to dissolve 42 mg of 2-chloroethylamine hydrochloride. Protein concentrations were verified on NanoDrop. The probe modification reaction was activated using 100 μL of 2 M NaOH and allowed to continue for 40 min at room temperature. Following this activation, the reactive probes were subjected to dialysis against reaction buffer (50 mM Tris, 50 mM NaCl, pH 7.4) using Slide-A-Lyzer cassettes (Thermo Scientific) for 1 h at room temperature.

Wild-type and mutant vOTU were diluted with deubiquitinating enzyme (DUB) buffer (25 mM Tris, 150 mM NaCl, 5 mM DTT, pH 8.0) to a final concentration of 0.5 mg/mL and incubated for 5 min at room temperature. In the reactions with each suicide probe, 20 μL of the given enzyme was mixed with 50 μL of the given suicide probe. 17 μL of the reaction was taken out at indicated timepoints and mixed with 10 μL of lauryl dodecyl sulfate (LDS) loading buffer (Invitrogen) to stop the reaction. 10 μL of each sample resolved on 4–12% SDS-PAGE gels and stained with Instant Blue (Expedeon).

Preparation of vOTU Complexes with Ub or ISG15 for Crystallization. For crystallography, complex formation of Ub and ISG15-C with vOTU was performed in reaction buffer (25 mM Tris, 200 mM NaCl, pH 8.0) for 1 h using 2× molar excess of suicide probe. The resulting covalent vOTU complexes were purified by cation-exchange chromatography (RESOURCE S) at pH 6.5 over a linear salt gradient to 500 mM NaCl. Gel filtration using a Superdex 75 16/60 column in reaction buffer with 5 mM DTT was used as the final step of purification. The complex protein was concentrated to 10 mg/mL for vOTU–Ub and 15 mg/mL for vOTU–ISG15 using a Vivaspin 10 K (Sartorius) concentrator and used in crystallization screening. The purity of both complexes were >95% pure as judged by Coomassie stained SDS-PAGE gel.

Crystallization. Initial hits for all crystals were obtained from nanoliter crystallization screening using sitting-drop setup. Optimization was performed using the hanging-drop vapor diffusion method. Crystals of vOTU were obtained from 3.9 M sodium formate as a reservoir solution at 20 °C. Crystals grew over 7 days. SeMet substituted protein crystallized under the same conditions. Prior to freezing in a nitrogen cryostream, crystals were soaked in mother liquor containing 5% glycerol. The vOTU–Ub complex crystallized from 0.27 M sodium dihydrogen phosphate, 1.53 M di-potassium hydrogen phosphate, pH 7.5 and crystals grew over 5 days. The vOTU–ISG15-C complex crystallized from 10% PEG 8000, 0.2 M zinc acetate, 0.1 M MES sodium salt (pH 6.5) and crystals grew over 2 weeks.

Data Collection, Structure Determination, and Refinement. Diffraction data were collected at beam lines ESRF ID14-4 and Diamond I-03 synchrotron as detailed in Table S1. All diffraction data was processed using iMosflm (3) and the CCP4 software suite (4). The structure of unliganded vOTU was determined by SAD phasing in autoSHARP (5) using data collected from a SeMet substituted crystal. Automated model building in ARP/WARP (6) traced ~85% of vOTU residues. Complex structures with Ub and ISG15 were determined by molecular replacement with PHASER (7) using the vOTU structure as well as Ub and ISG15 structures as search models. Further manual model building and refinement in Coot (8) and Phenix (9) resulted in final statistics shown in Table S1. All structures displayed well ordered electron density (Fig. S6).

Quantitative AMC Fluorescence Measurements. Ub-AMC and ISG15-AMC (Boston Biochem) were subjected to dialysis against AMC reaction buffer (50 mM Tris, 50 mM NaCl, pH 7.4) to remove excess free AMC in the samples and homogenize buffer for both probes. To derive kinetic constants of vOTU against both substrates, a dilution series of each AMC substrate was prepared that allowed Michaelis–Menten curve fitting. Triplicate measurements were done at each substrate concentration. In each reaction, 14 μL of substrate was added to a single well of a 384-well low volume plate (Corning), and the AMC hydrolysis was initiated by the addition of 5 μL of 4.75 nM vOTU (final vOTU concentration was 1.25 nM) at 37 °C. The reaction was monitored with a PheraStar plate reader (BMG Labtech) operating an optic module with excitation wavelength at 340 nm and emission wavelength at 440 nm. The true concentration of each diluted substrate was determined from the complete hydrolysis of the diluted substrates at various concentrations and compared the fluorescence values to a linear standard curve using free AMC at various known concentrations. Progess curves at various substrate concentrations were obtained by monitoring fluorescence intensity as a function of time. The curves were fitted to a first order exponential decay function and converted to a molar concentration scale using the standard curve. Initial rates at the various concentrations were then determined by taking the slope at $t = 0$. Initial rates were plotted against substrate concentration and fitted to the Michaelis–Menten equation within Prism 5 (Graphpad). The K_m values were taken into account when comparing the activity between wild-type and mutant vOTU against Ub- and ISG15-AMC. The procedure for these reactions were as described above. The final substrate concentrations in these measurements were determined to be 220–240 nM, significantly below the K_m, whereas the final enzyme concentrations were increased to 75 nM.

Purification of Ubiquitin and Generation FlAsH-Tagged Ub Dimers. Ubiquitin molecules carrying a K63R mutation or a C-terminal FlAsH-tag (W-C-C-P-G-C-C), replacing ubiquitin residues 72–76, were expressed in *E. coli* Rosetta2 pLysS (Novagen) cells and purified according to ref. 10. The additional Trp residue preceding the FlAsH-tag sequence allowed a reliable measurement of ubiquitin concentration. The cleared cell lysates were loaded onto a HiLoad Sepharose cation-exchange column (GE Life Sciences) and separated using a linear salt gradient containing 50 mM NH_4Ac pH 4.5 (Buffer C) and Buffer C + 1 M NaCl (Buffer D). The peak fractions containing ubiquitin were pooled and concentrated to a volume suitable for loading onto a gel filtration column (Superdex 16/60, GE Life Sciences) in buffer E (50 mM Tris pH 7.6). The ubiquitin K63R mutant was >95% pure after gel filtration, as judged by SDS-PAGE gel. For ubiquitin mutant carrying the FlAsH-tag, a further separation step on a MonoS cation-exchange column (GE Life Sciences) was required, employing Buffer C and Buffer D in a linear salt gradient.

Ligation and purification of K63-linked ubiquitin dimers was performed according to ref. 10. Purified ubiquitin dimers were labeled with Lumio Green Reagent (Invitrogen) according to manufacturer's protocol. 10 nmol of K63-linked ubiquitin dimers was used in a reaction with 10 μL of Lumio Green for 1 h at room temperature, followed by overnight dialysis against Buffer F (50 mM Tris, 50 mM NaCl, 0.1% (v/v) β-mercaptoethanol, pH 7.6). The final concentration of labeled ubiquitin dimer was determined by NanoDrop at 515 nm using the extinction coefficient value of $4.1 \times 10^4\ M^{-1}\ cm^{-1}$.

Quantitative Fluorescent Anisotropy Assay. Fluorescent diubiquitin molecules were stepwise diluted down to a series of concentrations spanning a range that allowed Michaelis–Menten plot fitting. In each case, 10 μL of 2-fold concentrated substrate was prepared in individual wells of a 384-well plate (Corning) and the reactions were initiated by addition of 10 μL of 2 nM vOTU. The change in fluorescence anisotropy was monitored with a PHERAstar (BMG Labtech) plate reader carrying an FP optic module with excitation wavelength at 485 nm and emission wavelength at 520 nm. The reaction was carried out at 37 °C for a length of time that allowed data fitting to a single phase decay, typically less than 10 min. At each substrate concentration, triplicate deubiquitination reactions were measured, and a final Michaelis–Menten curve could be plotted from the initial rates of reactions, which was in turn derived from the first order differentiation of concentration normalized decay curves at $t = 0$. All curve fitting was done in GraphPad Prism.

Qualitative Deubiquitination Assays. The concentrations of ubiquitin dimers of K6, K11, K29, K48, K63, and linear linkages were determined by NanoDrop at the linear range measurement at 280 nm. The ubiquitin substrates were subsequently diluted stepwise down a final concentration of 0.5 mg/mL. The procedures for this assay have previously been reported (11). For each deubiquitinase reaction, 3 μL of the ubiquitin dimers was added to 14 μL of H_2O, plus 3 μL of 10 × DUB buffer. The vOTU constructs were diluted in the DUB buffer to the final concentration of 0.2 μg/mL and 10 μL of the indicated vOTU construct was added to each of the preprepared solutions containing different ubiquitin dimers. At the given timepoints, 6 μL of the reaction sample was taken out and the reaction was stopped by mixing with 5 μL of LDS buffer. The samples were separated on 4–12% SDS-PAGE gels and visualised using silver staining according to manufacturer's protocol (Invitrogen).

Generation of Ubiquitinated and ISGylated Model Substrates. Polyubiquitinated UBE2S was generated according to ref. 12. 4 μL of polyubiquitinated UBE2S was incubated with 5 μL of wild-type or mutant vOTU at 0.2 μg/mL for 1 h at 37 °C. The reactions were stopped by addition of 6 μL LDS sample buffer (Invitrogen) and resolved on a 4–12% SDS-PAGE gel. Western-blot analysis using rabbit polyclonal antiUb (Millipore) was carried out according to ref. 12.

Protein ISGylation was induced according to ref. 13. HeLa cells were stimulated with IFN-β at 1000 units/mL (Betaseron) and incubated for 24 h at 37 °C. The stimulated cells were subsequently lysed in 500 μL of lysis buffer (150 mM NaCl, 30 mM Tris HCl pH 7.4, 2 mM ethylenediaminetetraacetic acid (EDTA) 10 glycerol, 1 mM sodium orthovanadate, 1 mM NaF, 0.5 % NP40) using standard protocols. The lysate was centrifuged in a benchtop centrifuge at 13200 rpm for 10 min at 4 °C and the supernatant was transferred into a prechilled test tube. 5 μL of wild-type or mutant vOTU at 2 μg/mL was used to incubate with 10 μL of cell lysate for 1 h at 37 °C. The reaction was stopped and visualized by Western blot in the same manner as described above. ISG15 modifications were visualized by Western blotting using a mouse polyclonal anti-ISG15 antibody (H-150, SantaCruz).

1. Berrow NS, et al. (2007) A versatile ligation-independent cloning method suitable for high-throughput expression screening applications. *Nucleic Acids Res* 35:e45.
2. Borodovsky A, et al. (2002) Chemistry-based functional proteomics reveals novel members of the deubiquitinating enzyme family. *Chem Biol* 9:1149–1159.
3. Leslie AG (2006) The integration of macromolecular diffraction data. *Acta Crystallogr D* 62:48–57.
4. CCP4 (1994) The CCP4 suite: Programs for protein crystallography. *Acta Crystallogr D* 50:760–763.
5. Bricogne G, Vonrhein C, Flensburg C, Schiltz M, Paciorek W (2003) Generation, representation, and flow of phase information in structure determination: Recent developments in and around SHARP 2.0. *Acta Crystallogr D* 59:2023–2030.

6. Perrakis A, Morris R, Lamzin VS (1999) Automated protein model building combined with iterative structure refinement. *Nat Struct Biol* 6:458–463.
7. McCoy AJ, Grosse-Kunstleve RW, Storoni LC, Read RJ (2005) Likelihood-enhanced fast translation functions. *Acta Crystallogr D* 61:458–464.
8. Emsley P, Cowtan K (2004) Coot: Model-building tools for molecular graphics, *Acta Crystallogr D* 60:2126–2132.
9. Adams PD, et al. (2002) PHENIX: Building new software for automated crystallographic structure determination. *Acta Crystallogr D* 58:1948–1954.
10. Pickart CM, Raasi S (2005) Controlled synthesis of polyubiquitin chains. *Methods Enzymol* 399:21–36.
11. Komander D, et al. (2009) Molecular discrimination of structurally equivalent Lys 63-linked and linear polyubiquitin chains. *EMBO Rep* 10:466–473.
12. Bremm A, Freund SM, Komander D (2010) Lys11-linked ubiquitin chains adopt compact conformations and are preferentially hydrolyzed by the deubiquitinase Cezanne. *Nat Struct Mol Biol* 17:939–947.
13. Durfee LA, Lyon N, Seo K, Huibregtse JM (2010) The ISG15 conjugation system broadly targets newly synthesized proteins: Implications for the antiviral function of ISG15. *Mol Cell* 38:722–732.

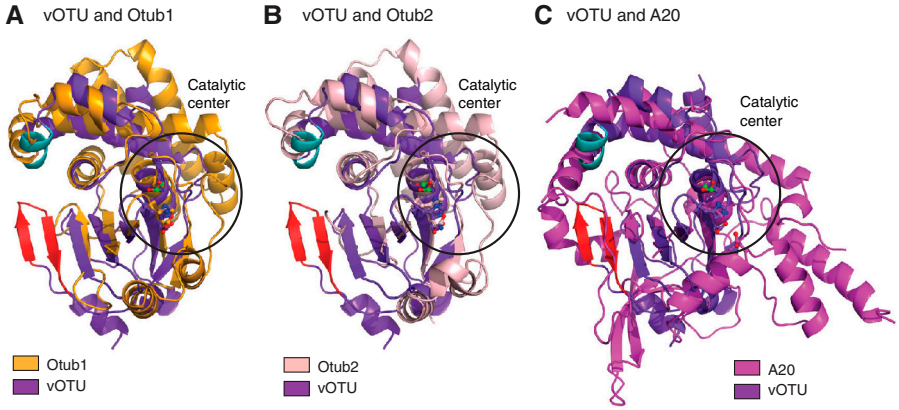

Fig. S1. Superposition of vOTU with mammalian OTU domains. (*A*) Superposition of vOTU (purple, colored as in Fig. 2*A*) and Otub1 [orange; Protein Data Bank (PDB) ID 2ZFY (1)] in cartoon representation. The vOTU is in the same orientation as in Fig. 2*A*. Catalytic site residues are shown in ball-and-stick representation. (*B*) Superposition of vOTU and Otub2 [PDB ID 1TFF (2)]. (*C*) Superposition of vOTU and A20 [magenta; PDB ID 2VFJ (3)].

1 Edelmann MJ, et al. (2009) Structural basis and specificity of human otubain 1-mediated deubiquitination. *Biochem J* 418:379–390.
2 Nanao M, et al. (2004) Crystal structure of human otubain 2. *EMBO Rep* 5:783–788.
3 Komander D, Barford D (2008) Structure of the A20 OTU domain and mechanistic insights into deubiquitination. *Biochem J* 409:77–85.

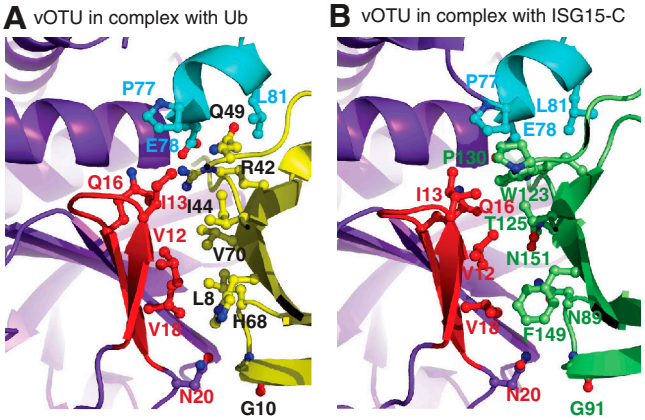

Fig. S2. Close-up view of interactions between vOTU and Ub/ISG15-C. (*A*) Structure of vOTU in complex with Ub labeled as in Fig. 3*A*. Residues mediating the interactions are shown in ball-and-stick representation and labeled. (*B*) Structure of vOTU in complex with ISG15-C labeled as in Fig. 3*B*, and in the same orientation as in (*A*).

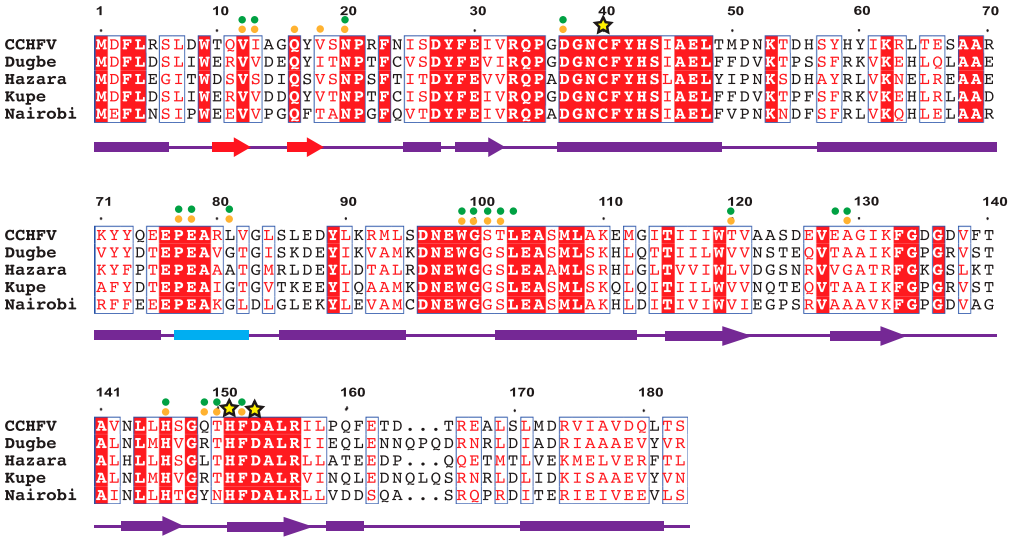

Fig. S3. Full sequence alignment and secondary structure of the vOTU region from CCHFV, Dugbe virus, Hazara virus, Kupe virus, and Nairobi sheep disease virus as in Fig. 4. Boxes and arrows above the sequence show α-helical and β-strand regions of CCHFV, respectively. Yellow stars indicate catalytic residues. Identical residues are highlighted in red. Residues involved in interaction with Ub or ISG15 are indicated by orange or green dots, respectively.

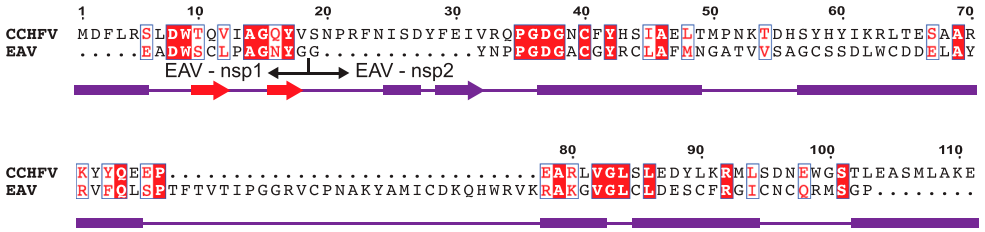

Fig. S4. Sequence alignment of CCHFV vOTU with EAV nsp2. Sequence alignment with secondary structure elements indicated for the N-terminal regions of the CCHFV vOTU and EAV nsp2 protein. Secondary structure of CCHFV is represented in the same way as in Fig. S3. Whereas an N-terminal extension would be cleaved off (the boundary according to ref. 1 is indicated), an insertion predicted to be within the helical arm of EAV nsp2 may contribute to the S1 Ub binding site.

1 Ziebuhr J, Snijder EJ, Gorbalenya AE (2000) Virus-encoded proteinases and proteolytic processing in the Nidovirales. *J Gen Virol* 81:853–879.

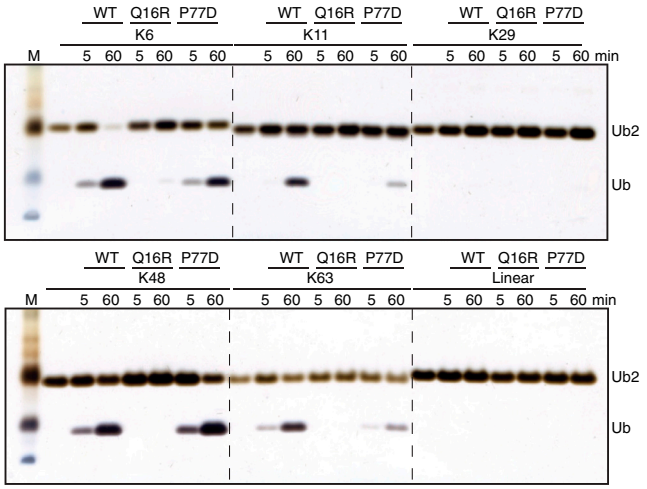

Fig. S5. Qualitative linkage specificity analysis of vOTU and mutants against diubiquitin of different linkages. Samples of 5 μL were taken from a reaction at indicated time points, resolved on a 4–12% SDS-PAGE gel and silver stained, as in Fig. 1*D*.

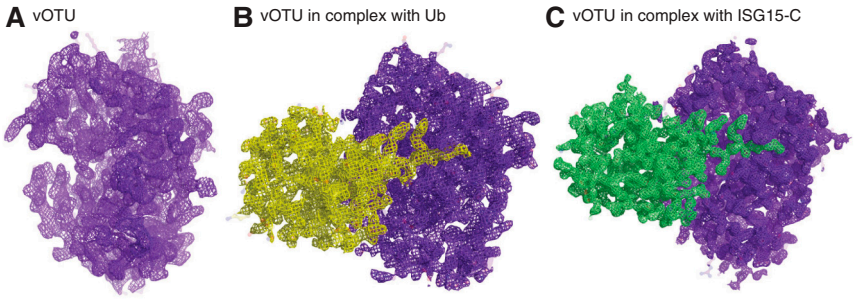

Fig. S6. Electron density of crystal structure of vOTU, in complex with Ub and ISG15-C. (*A*) Weighted 2|Fo|-|Fc| electron density contoured at 1σ of vOTU (purple) in same orientation as Fig. 2*A*. (*B*) vOTU (purple) in complex with ubiquitin (yellow). (*C*) vOTU (purple) in complex with ISG15-C.

Table S1. Crystallization data collection and refinement statistics

	vOTU Apo, SeMet	vOTU_Apo	vOTU–Ub	vOTU–ISG15-C
Data collection statistics				
Beamline	Diamond I-03	ESRF ID14-4	ESRF ID14-4	ESRF ID14-4
Wavelength (Å)	0.9800	0.9795	0.9795	0.9800
Space group	$P322_1$	$P322_1$	$P2_12_12_1$	$P2_1$
Unit cell (Å)	$a, b = 115.71$ $c = 95.65$	$a, b = 115.99$ $c = 94.17$	$a = 79.44$ $b = 106.17$ $c = 111.46$	$a = 41.52$ $b = 37.10$ $c = 84.35$ $\beta = 94.24$
Resolution (Å)	69.19-3.10(3.27-3.10)	50.22-2.20(2.32-2.20)	49.34-2.00 (2.11-2.00)	38.29-1.60(1.69-1.60)
Observed reflections	99424 (14813)	201872 (29887)	145270 (21229)	110331 (15829)
Unique reflections	13807 (1999)	37465 (5417)	59820 (8988)	33549 (4845)
Redundancy	7.2 (7.4)	5.4 (5.5)	2.4 (2.4)	3.3 (3.3)
Completeness (%)	100.0 (100.0)	99.9 (100.0)	94.0 (97.	98.1 (97.5)
R_{merge}	0.101 (0.363)	0.074 (0.497)	0.104 (0.318)	0.063 (0.351)
$\langle I/\sigma I \rangle$	13.7 (5.0)	13.7 (3.5)	6.4 (3.1)	11.6 (3.1)
Phasing statistics				
FOM	0.329			
FOM after DM	0.864			
Refinement statistics				
Reflections in test set		1823	2925	1607
R_{cryst}		19.4	21.3	14.0
R_{free}		23.1	27.8	19.2
Number of groups				
Protein atoms		2942	7493	1930
Ions and ligand atoms		6	0	20
Water		143	562	192
Rmsd from ideal geometry				
Bond length (Å)		0.013	0.005	0.016
Bond angles (°)		1.488	0.903	1.395
Ramachandran plot statistics				
In favored regions (%)		339 (94.2)	891 (97.7)	234 (98.7)
In allowed regions (%)		21 (5.8)	21 (2.3)	3 (1.3)
Outliers (%)		0 (0)	0 (0)	0 (0)

Values in parentheses are for the highest resolution shell.